IJST, Transactions of Civil Engineering, Vol. 39, No. C2, pp 299-317
Printed in The Islamic Republic of Iran, 2015

SEMI-ACTIVE FUZZY CONTROL OF STRUCTURES SUBJECTED TO NEAR-FAULT GROUND MOTIONS HAVING FORWARD DIRECTIVITY AND FLING STEP USING FRICTION DAMPING SYSTEM WITH AMPLIFYING BRACES (FDSAB)*

H. GHAFFARZADEH[1**], E. ALIZADEH DEHROD[2] AND H. AGHAYI PAR[3]

[1]Dept. of Civil Engineering, University of Tabriz, Tabriz, I. R. of Iran
Email: ghaffar@tabrizu.ac.ir
[2]Dept. of Civil Engineering, Science and Research Branch of Islamic Azad University, Tehran, I. R. of Iran
[3]Dept. of Civil Engineering, Islamic Azad University of Boukan, West Azerbaijan, I. R. of Iran

Abstract– In this paper, the consequences of well-known characteristics of near-fault ground motions, forward directivity and fling step, on the seismic response control is investigated. An integrated fuzzy rule-based control strategy for building structures incorporated with semi active friction damping system with amplifying braces (FDSAB) is developed. The membership functions and fuzzy rules of fuzzy controller were optimized by Genetic Algorithm (GA). The main purpose of employing a GA is to determine appropriate fuzzy control rules as well to adjust parameters of the membership functions. Numerical study is performed to assess the effects of near-fault ground motions on a building that is equipped with FDSABs. To demonstrate the effectiveness of the fuzzy logic algorithm, it is compared with that of a conventional linear quadratic regulator (LQR) controller, while the uncontrolled system response is used as the base line. Results reveal that the fuzzy logic controller with FDSAB is capable of improving the structural responses and is promising for reducing seismic responses during near-fault earthquakes. It is also shown that, the near-fault earthquakes require much more control force than the far-field earthquakes and result in less response mitigation.

Keywords– Near-fault ground motions, semi-active control, FDSAB, fuzzy logic controller (FLC), genetic algorithm (GA), linear quadratic regulator (LQR)

1. INTRODUCTION

Structural control strategies have been a subject of intensive research and have been recognized as a promising approach for response suppression in recent decades. Structural control systems can be classified to active, semi-active and passive control methods. Semi-active structural control not only maintain the reliability of passive control systems, but also provide the versatility of active control systems with a much lower power requirement which is of great importance in structural control during earthquakes [1].

Among many semi-active control devices [2, 3], semi-active friction damping systems with amplifying braces (FDSAB) are more attractive to use because of mechanical simplicity, small size and low operating power requirement. Additionally, the control forces required when FDSAB are used are smaller compared with structures controlled by friction dampers connected either to chevron or diagonal braces [4]. This makes FDSAB more effective to use in structural control, especially for structures that may be subjected to severe earthquakes.

*Received by the editors March 15, 2013; Accepted March 4, 2014.
**Corresponding author

The control effectiveness of structural systems is highly dependent on the control strategy used for designing semi-active control law. Conventional control algorithms are reliant on having an accurate model of the system [2, 5, 6, 7, 8]. Although these model-based strategies have been successful in suppression of structural vibrations, they suffer from some inherent shortcomings for structural applications and their performance is strongly affected by the accuracy of the model selected. The other approaches, as alternatives to the classical control algorithms, consist of methods which do not rely on a system model. They are based on the actual measured responses of the system. This category includes neural network and fuzzy control methods [9-13].

Fuzzy logic control (FLC) theory for vibration control of structural systems has attracted the attention of researchers due to inherent robustness, ease in handling the uncertainties, nonlinearities and heuristic knowledge. FLC allows the resolution of imprecise or uncertain information. Moreover, the computations for driving the controller are quite simple, and can be easily implemented into a fuzzy chip [14]. Fuzzy control systems have been successfully applied to wide variety of control problems. A semi-active fuzzy control strategy for seismic response reduction using a magneto-rheological (MR) damper has been proposed by Choi et al [12]. A fuzzy rule-based semi-active control of building frames using semi-active hydraulic dampers (SHDs) was presented by Bidokhti et al [15]. Ozbulut and Hurlebaus [16] proposed fuzzy logic controllers for operating control force of piezoelectric friction dampers used for seismic protection of base-isolated buildings against various types of earthquake excitations.

In structural control applications, GA can be utilized as an optimization technique to pursue the ultimate goal of reducing the structural responses that determines the structural safety. In design of FLC, choosing appropriate membership functions is a significant and time-consuming part. Some valuable efforts were achieved towards the application of a genetic algorithm (GA) to the design of a FLC [16]. In this manner, the GA optimized FLC is used to adjust the parameters of the fuzzy membership functions and finding appropriate fuzzy control rules.

Near-fault ground motions impose large demands on structures compared to ordinary ground motions. The damaging effects of near-field motions on civil structures have emphasized the need for innovative design strategies. The intense dynamic motions are caused by normal component of the near-field motions, forward rupture directivity, which is commonly characterized by a long-period velocity pulse. The fault-parallel component of the near-fault ground motions, fling step, is special aspect of near-fault ground motions that usually induces only limited inertial demands on structures due to the long-period nature of the static displacement [17]. Effect of near-fault ground motions on semi-active control algorithm by variable orifice and MR dampers was investigated by Ghaffarzadeh et al [18,19]. They concluded that the near-fault earthquakes require much more control force than the far-field earthquakes and result in less response mitigation.

Consequently, due to different characteristics of ground motions, an optimal controller should be developed to drive a semi-active damper for both far-field and near-field earthquakes. Actually, incorporation of forward directivity and fling step effects into the design of fuzzy logic controller is questionable. This paper aims at evaluation of fuzzy logic control strategy adopted for seismic protection and the selected semi-active system, FDSAB, when the structural system is subjected to near-fault ground motions with forward directivity and fling step effects. In fact, effect of earthquake intensity on the seismic performance of controlled structural system is assessed in relation to the characteristics of the near-fault ground motions. In other words, the focus of this study is the potential for near-fault effects associated with forward-directivity and fling step effects, and how these near-fault effects can affect the response control and its algorithm. Displacement and velocity responses are considered as the feedback to the fuzzy logic controller. Genetic algorithm technique was utilized to design an accurate fuzzy controller by optimization of the membership functions and fuzzy rules of fuzzy controller. In a numerical example,

the developed FLC is applied to a ten story building and time history analyses are conducted to evaluate the performance under characteristics of near-fault ground motions. Furthermore, the results are compared with those of linear quadratic regulator (LQR) control algorithm to demonstrate the efficiency of fuzzy logic controller.

2. FRICTION DAMPING SYSTEM WITH AMPLIFYING BRACES

Over the past few years, friction dampers have been widely investigated as an energy dissipation system to mitigate the structural response due to dynamic loading [1]. In this study, FDSAB system is used as semi active device for vibration control of structure. The other feature of FDSAB device is its large amount of dissipated energy at each cycle of loading. The friction damping system with amplifying braces (FDSAB) is a semi active device that consists of a square frame (1), with bars connected by hinges (2a, 2b, 2c and 2d), a system of cables (3) and a semi-active friction damper (4) as shown in Fig 1a [4]. The proposed friction damper is shown in Fig 1b which consists of an external cylinder (5), two internal half-cylinders (6a and 6b) and a pneumatic camera (7). The damper is connected to the top and bottom floor diaphragms by means of cables (3).

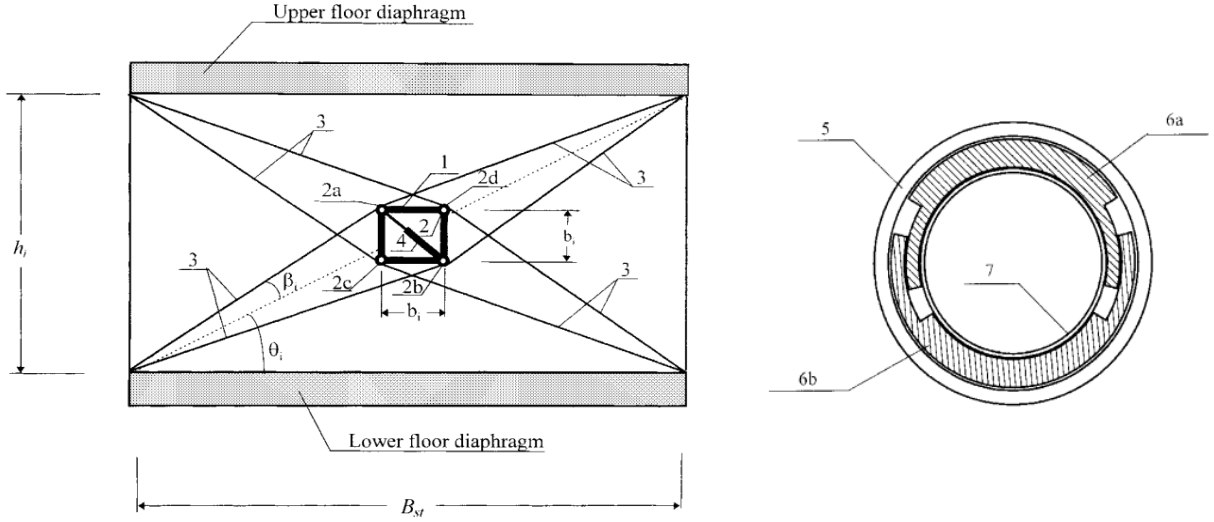

(a) (b)

Fig. 1. FDSAB Device (a) Construction scheme, (b) Construction scheme of a friction damper [4]

In FDSABs, the air pressure in the pneumatic camera of each damper adjusts the slip force level according to the optimal solution yielding the required friction forces based on control algorithm. Typical force–displacement hysteretic loop for a friction damper has rectangular shape. Assuming that the cable length remains constant, the amplified displacement transferred to the FD at each floor level i takes the form:

$$d_{FD,i} = \frac{b_i^* - \sqrt{\left(b_i^*\right)^2 - 4c_i^*}}{2} \tag{1}$$

where $b_i^* = 2\sqrt{2}b_i$, $c_i^* = 2B_{st,i}d_i\cos\theta_i + d_i^2\cos^2\theta_i$ in which B_{st} is the storey bay, b_i is the dimension of the square, d_i is the storey drift of *i*th floor. The energy dissipated at the *i*th floor is given by:

$$E_i = d_{FD,i}F_{FD,i} \tag{2}$$

where $F_{FD,i}$ is the control force at the *i* th floor.

3. NEAR-FAULT GROUND MOTIONS

Failures of modern engineered structures observed within the near-fault regions disclosed the significance of near-fault ground motions. These motions are defined as the area in the proximity of the fault rupture surface and are strikingly different than those observed further away from the seismic source. They may generate high demands that force the structures to dissipate this input energy with few large displacement excursions.

a) Forward directivity effect

Forward-directivity effects are commonly characterized by a long-period velocity pulse acting normal to the fault and cause intense, coherent dynamic motions. Forward-directivity effects are seen when the rupture direction is aligned with the direction of slip, and the rupture front moves towards a given site at a velocity nearly equal to the propagation velocity of the shear waves. It has been reported that the period of a directivity pulse increases with the magnitude of the earthquake [20]. These motions have, on average, larger elastic spectral acceleration values at moderate to long periods. Evaluation of the velocity–time histories and displacement–time histories of these motions reveals the special nature of the pulse-like motion due to forward directivity. Forward directivity effects in the near-fault region can cause large-amplitude pulses that occur early in the velocity time history [21].

b) Fling step

On the other hand, fling step is produced due to permanent ground displacements associated with rupture mechanism. Pulses from fling-step have different characteristics than forward-directivity pulses. Near-fault fling types of records are generally characterized with a unidirectional large-amplitude velocity and a monotonic in the displacement time history. This permanent displacement of the ground resulting from fault rupture can be important for structural design [17].

c) Selection of ground motions

The considered ground motions constitute both near-fault and far-fault ground motions to specifically study the FDSAB performance in relation to the characteristics of the near-fault ground motion. Near-fault records were chosen so as to consider the presence of both forward directivity and fling step effects. Three near-fault ground motion records characterized with forward directivity and three near-fault ground motions characterized with fling step were selected. In contrast, another set of earthquake records at the same site was selected to illustrate ordinary far-field ground motion characteristics. Table 1 lists basic characteristics of the recorded motions. Figures 2 and 3 illustrate ground acceleration time history for the selected fault-normal component of near-fault ground motions having forward directivity and ground acceleration time histories of fault-parallel component having fling step, respectively. It can be seen that these typical near-fault records have an apparent acceleration pulse that induces very large displacement. Ordinary far-fault ground motions without pulse are plotted in Fig 4. As noted in the previous section, evaluation of the velocity–time histories and displacement–time histories of near-fault motions reveals their special features. Ground acceleration, velocity and displacement time history traces of the Imperial Valley record associated with forward directivity effect and Chi-Chi (TCU068NS) record having fling step effect are illustrated in Fig 5 and Fig 6, respectively. As indicated particularly by the velocity and displacement traces, the records contain large-amplitude pulses. The fling step effect exhibits obvious tectonic deformation at the end of the displacement time history. Such pulses do not appear in a typical far-fault ground motion as shown for the Northridge (WST 270) record in Fig 7.

Table 1. Properties of selected ground motions

Type	Earthquake	Station	d (km)	PGA (g)	PGV (cm/s)	PGD (cm)
Forward Directivity Pulses	Imperial Valley	H-E0230	0.6	0.439	109.8	44.74
	Northridge	SCS052	6.2	0.612	117.4	52.47
	Northridge	TCU102NS	1.19	0.838	71.5	107.2
Fling Step Pulses	Chi-Chi	TCU102NS	1.19	0.171	71.5	107.2
	Chi-Chi	TCU068NS	3.01	0.365	292.2	867.7
	Chi-Chi	TCU068EW	3.01	0.505	280.5	709.5
Without Pulse	Northridge	WST270	29.0	0.361	20.9	4.27
	Northridge	CEN155	30.9	0.465	19.3	3.48
	Loma Prieta	WAH090	16.9	0.638	38.0	5.85

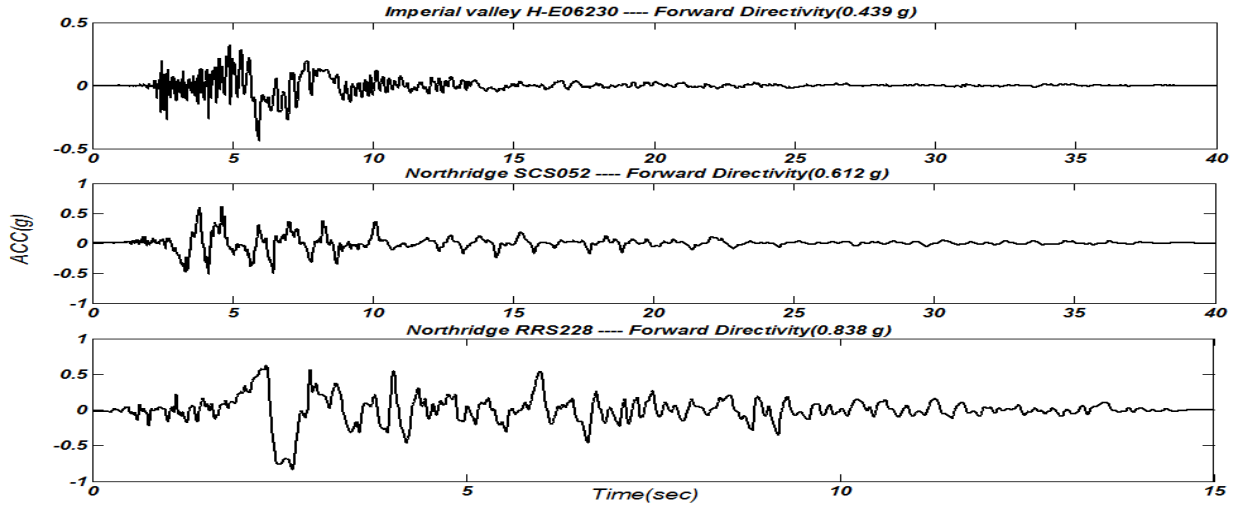

Fig. 2. Near-fault ground motions having forward directivity effects

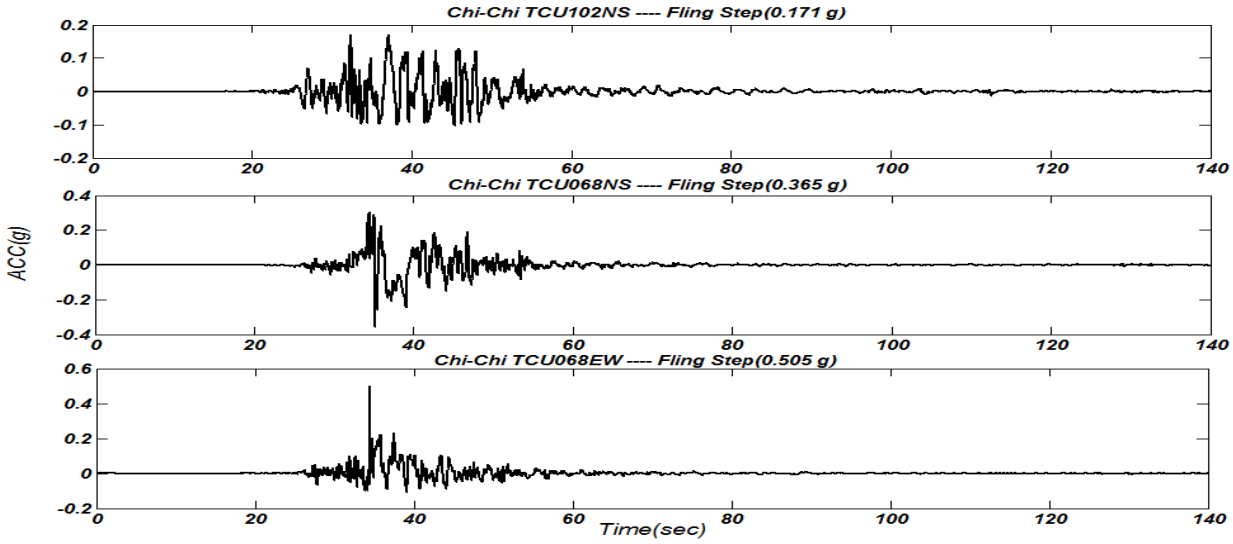

Fig. 3. Near-fault ground motions having fling step effects

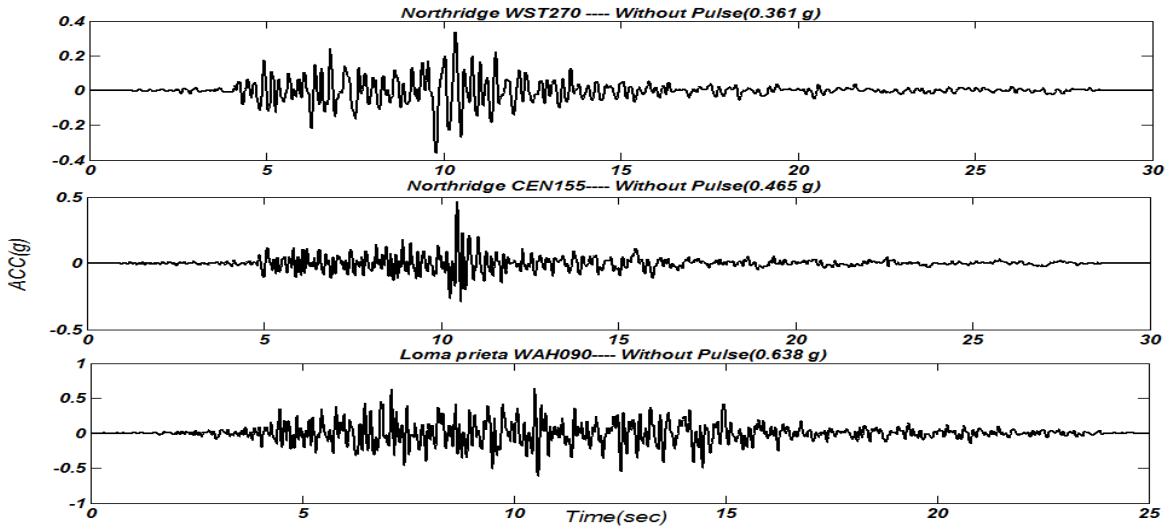

Fig. 4. Far- fault ground motions without pulse

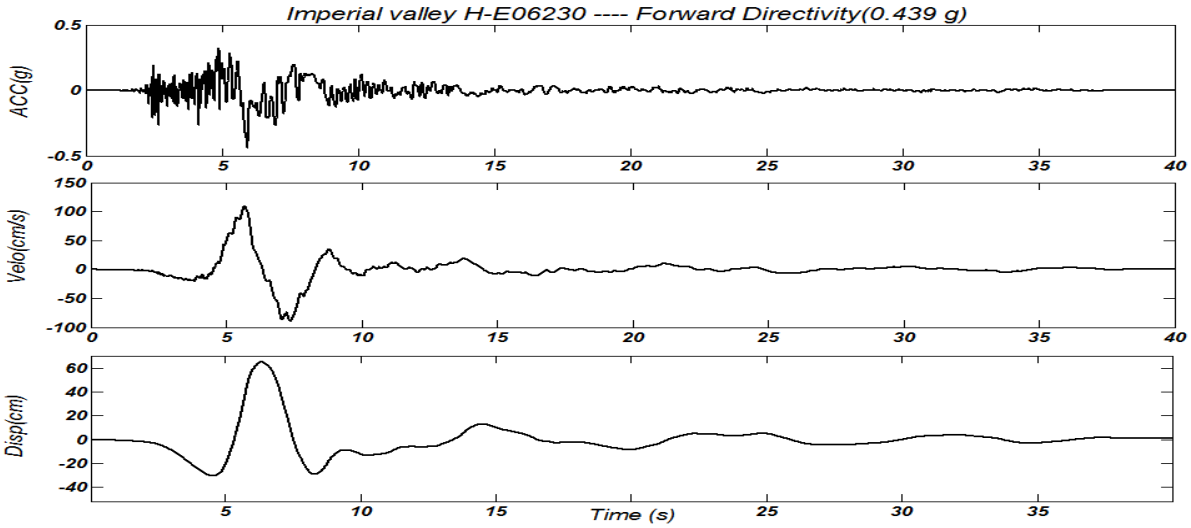

Fig. 5. Ground acceleration, velocity and displacement time histories of typical near-fault ground motions having forward directivity

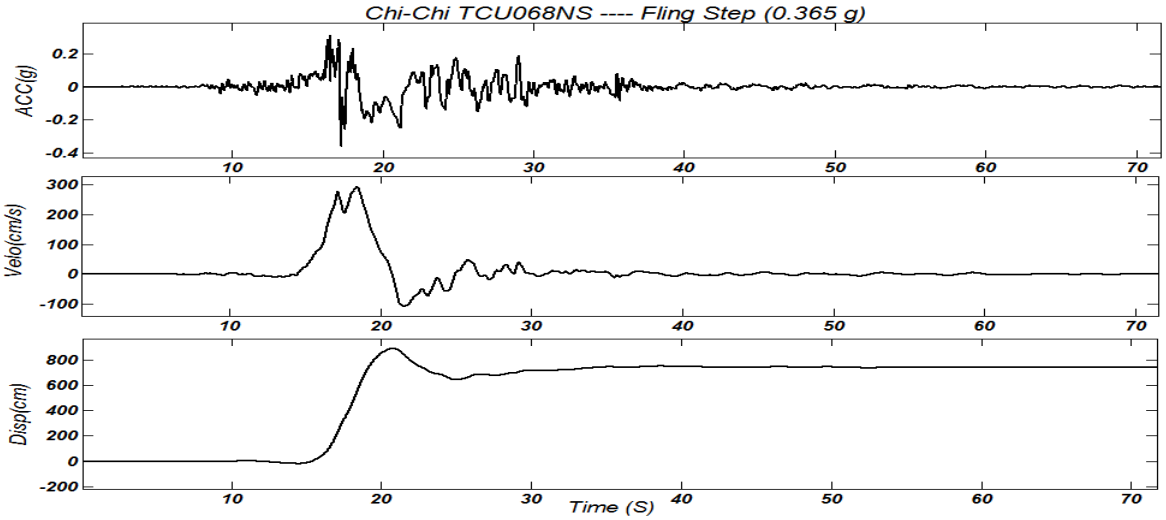

Fig. 6. Ground acceleration, velocity and displacement time histories of typical near-fault ground motions having fling step

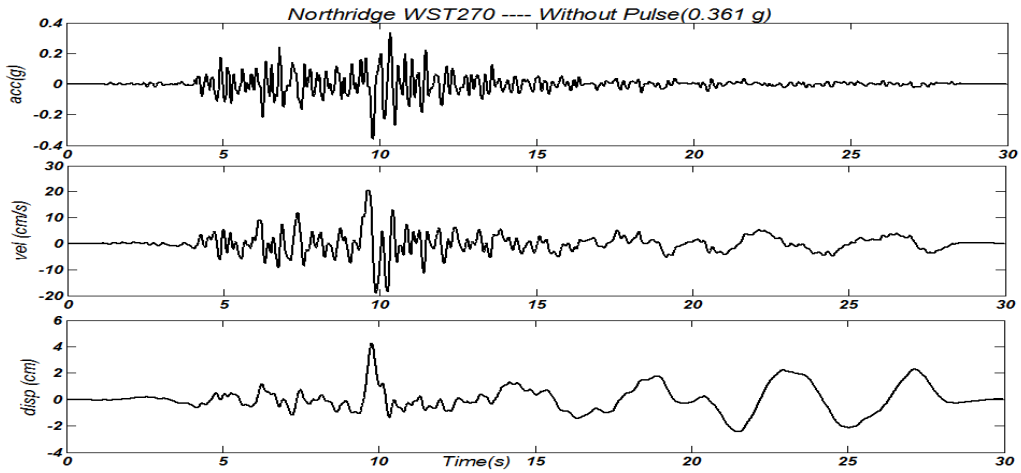

Fig. 7. Ground acceleration, velocity and displacement time histories of typical far-fault ground motions without pulse

4. LINEAR QUADRATIC REGULATOR CONTROL METHOD

The classical linear quadratic regulator algorithm (LQR) has been extensively used for semi active control. This control method requires that all the values of the state variables be available. In this algorithm, the control force u(t) is determined by minimizing the performance index over duration of excitation. In design process of LQR control algorithm, the equations of motion of a structure controlled with n dampers can be written as [22]:

$$[M]\{\ddot{x}(t)\}+[C]\{\dot{x}(t)\}+[K]\{x(t)\}=-[M]\{\Gamma\}\ddot{x}_g+[\Lambda]\{f(t)\} \tag{3}$$

where M, K and C represent the N ×N mass, structural stiffness and inherent structural damping matrices, respectively; x is a vector of the relative displacements of the floors of the structure, $\ddot{x}_g$ is a one dimensional ground acceleration, f = [f1 , f2 , … fn]^T is the vector of measured control forces corresponding to n number of FDSABs, Γ is a column vector of ones, and Λ is a vector determined by the placement of the dampers in the structure . This equation can be written in state-space form as:

$$\dot{z} = Az + Bf + E\ddot{x}_g \tag{4}$$

where z is the state vector, A is system matrix, B and E are force location matrices. A discrete-time linear system is defined by:

$$x(k+1) = Ax(k) + Bu(k) \tag{5}$$

In this system, the optimal control force takes the form u(k) = − G× x(k). G is a m × 2(n + m) feedback gain matrix where n is the number of stories and m is the number of FDSAB systems applied to control the building responses. This optimal control force is obtained by minimizing the performance index given by:

$$J = \sum_{k=0}^{\infty}(x^T(k)Qx(k) + u^T(k)Ru(k)) \tag{6}$$

where the symmetric weighting matrices Q and R are the weighting matrices to be applied to the response and control energy respectively. Q is a 2(n + m) × 2(n + m) positive semi-definite matrix; and R is a m × m positive definite matrix, which are defined as follows:

$$Q = [I]_{2N\times 2N} \quad , R = 10^{-12}[I]_{N\times N} \tag{7}$$

The control force u(k) is weighted in the performance index to allow regulation without using excessive control energy. Control force vector u(k) regulated by state vector x(k) is determined as:

$$u(k) = -G\,x(k) = -((R + B^T PB)^{-1} B^T PA)x(k) \tag{8}$$

and

$$P = Q + A^T(P - PB(R + B^T PB)^{-1} B^T P)A \tag{9}$$

where G and P are the solution of the classical discrete time algebraic Riccati equation.

5. SEMI-ACTIVE FUZZY LOGIC CONTROL ALGORITHM

Fuzzy logic theory allows objects to have any degrees of membership between 0% and 100% while traditional mathematics requires objects to have either 0% or 100% membership. Instead of complicated mathematical terms, fuzzy logic uses simple verbose statements to describe relationships between inputs and outputs of a controller. Fuzzy logic control is a knowledge-based control strategy and enables the use of linguistic directions as a basis for control. Due to its simplicity and effectiveness, several researchers have used fuzzy logic theory to develop controllers for semi-active devices [23]. Figure 8 illustrates general architecture of a fuzzy logic controller. The design of a fuzzy logic controller involves four main steps. The first step is fuzzification. After defining input and output variables that will be applied, input variables are transformed into linguistic variables by assigning membership functions to each input and output variable. In the second step, a rule base that relates the inputs to output by means of if–then rules is defined. An inference engine is then defined that evaluates the rules to produce the system output. The performance of a conventional FLC depends on various controller parameters such as the scaling factors, the membership functions, and the rule base. An effective rule base to perform at the desired level is more significant in FLC. The final step is defuzzification, where the output variable that is a fuzzy quantity is transformed to a non-fuzzy discrete value. In fact, the defuzzification module combines a set of fuzzified outputs for all the rules in order to arrive at a single conclusion. This paper adopts the center-of-gravity (COG) method among the defuzzification methods. For the j-th rule of the i-th damper, the COG method is defined as:

$$y_i = \frac{\sum_{j=1}^{N_R} b_i^{(j)} \int \mu_i^{(j)}}{\sum_{j=1}^{N_R} \int \mu_i^{(j)}} \tag{10}$$

where NR is the number of rules applied to the given input, μi (j) is the output membership function corresponding to the fuzzy variable defined in the consequent statement of the jth rule for the ith input, bi(j) is the center of the output membership function μi (j), and $\int \mu_i^{(j)}$ represents the area of the output membership function μi (j). The initial membership functions for input and output vectors and rule base of the FLC are initially constructed by the skilled operators and updated in the next stage by GA to find proper required design parameters of the fuzzy space.

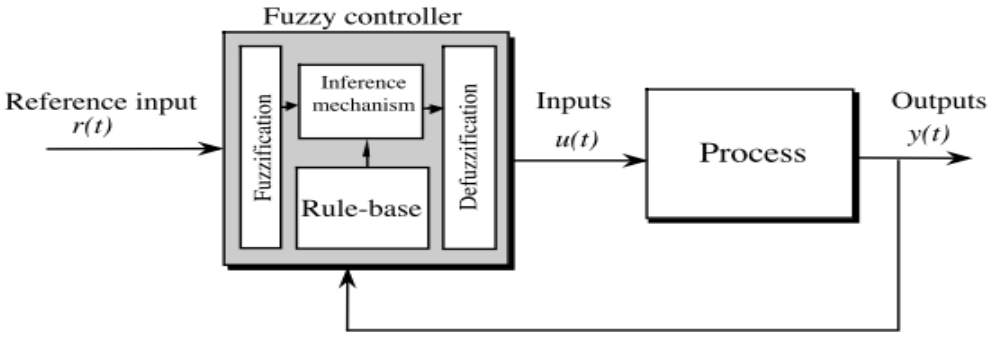

Fig. 8. Architecture of a fuzzy logic controller

a) Genetic algorithms

Many researchers have optimized FLC using a GA since Karr [24] first introduced a GA approach to design of FLCs. A genetic algorithm (GA) is a search technique that mimics biological evolutionary theories for optimization and search. The basic idea is to maintain a population of chromosomes that evolves over time through a process of competition and controlled variation. All of the information represented by the FLC parameters is encoded in a chromosome. Each chromosome is made up of a sequence of genes from binary digits (0 and 1) that represent design parameter values for each individual. GA starts with an initial population and uses operations of selection (reproduction), crossover, and mutation on a population of chromosomes to perform evolution to obtain improved solutions [25]. Each individual is assigned a fitness value and is chosen from the population, with a probability according to their relative fitness, for recombination to produce the next generation. Fitness function must be devised for each problem to be solved since it provides an important connection between the GA and the physical system that is being modeled. This fitness value reflects the performance of the solution and desired objectives. The fitness function to be minimized in this study is considered as:

$$F = \sum_{i=1}^{n} \left[\max\left(d_i \right) \right]^2 \tag{11}$$

where di is the controlled response of the building (here, the displacement response of the stories).

6. NUMERICAL EXAMPLE AND RESULTS

To evaluate the performance of the proposed semi-active fuzzy control system using FDSAB and its effectiveness in relation to characteristics of near-fault ground motions, forward directivity and fling step, a ten-story shear building structure is studied. Figure 9 illustrates the structural model for this study.

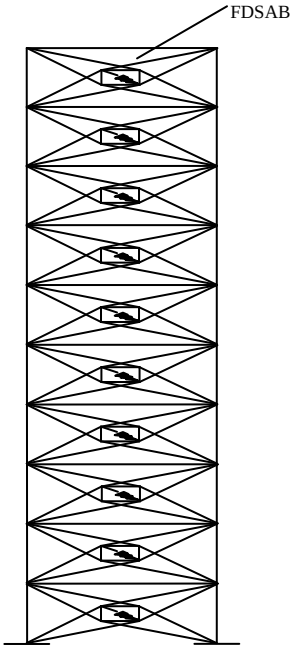

Fig. 9. Controlled test structure with FDSABs

a) Ten-story shear building

A model of a ten story building in which all stories are equipped with a FDSAB is considered. As stated earlier, the equation of motion of the ten storey shear building model, taken for seismic mitigation analysis is given in Eq. (3). Mass and stiffness parameters are listed in Table 2 and matrices are formed as

follows. The Rayleigh damping matrix is constructed using 3% modal damping for first and second modes.

$$M=\begin{bmatrix} m_1 & 0 & \cdots & 0 \\ 0 & m_2 & \cdots & 0 \\ \vdots & \vdots & \cdots & \vdots \\ 0 & 0 & \cdots & m_{10} \end{bmatrix} \quad , \quad K=\begin{bmatrix} k_1+k_2 & -k_2 & 0 & \cdots & 0 \\ -k_2 & k_{2+3} & -k_3 & \cdots & 0 \\ \vdots & \vdots & \vdots & \cdots & \vdots \\ 0 & 0 & 0 & & -k_{10} \end{bmatrix} \tag{12}$$

Table 2. Mass and stiffness values of test structure

Story	Mass	Stiffness
Story 1-3	95000 kg	1780×10^5 N/m
Story 4-6	87500 kg	1655×10^5 N/m
Story 7-9	77500 kg	1402×10^5 N/m
Story 10	65000 kg	1112×10^5 N/m

b) Design of fuzzy logic controller

The developed fuzzy logic controller consists of two input variable (displacement and velocity of stories), defined by seven membership functions defined on the normalized universe of discourse [−1, 1] and one output variable (control force) having eleven membership functions defined on the normalized universe of discourse [-1, 1]. A reasonable range of input values must be selected for the input membership functions since, if the range is too large or too small, the outermost membership functions will rarely or essentially be used, respectively, and thus limit the variability of the control system. The membership functions chosen for the input and output variables are triangular shaped, as illustrated in Fig 10. The definitions of the fuzzy variables of input membership function are as follows: NL = Negative Large, NM = Negative Medium, NS = Negative Small, ZR =Zero, PS = Positive Small, PM = Positive Medium and PL = Positive Large. The definitions of the fuzzy variables of the output membership function are as follows: NVL= Negative Very Large, NL = Negative Large, NM = Negative Medium, NS = Negative Small, NVS= Negative Very Small, ZR =Zero, PVS= Positive Very Small, PS= Positive Small, PM= Positive Medium, PL= Positive Large, PVL= Positive Very Large. The control force is the fuzzy control system output for the structural control system. Since normalized universes of discourse were used for both inputs and for the output to the fuzzy controller, scaling factors were required to map the variables to these domains. In this paper 20, 2 and 400000 N were selected as constant scaling factors of displacement, velocity and control force, respectively.

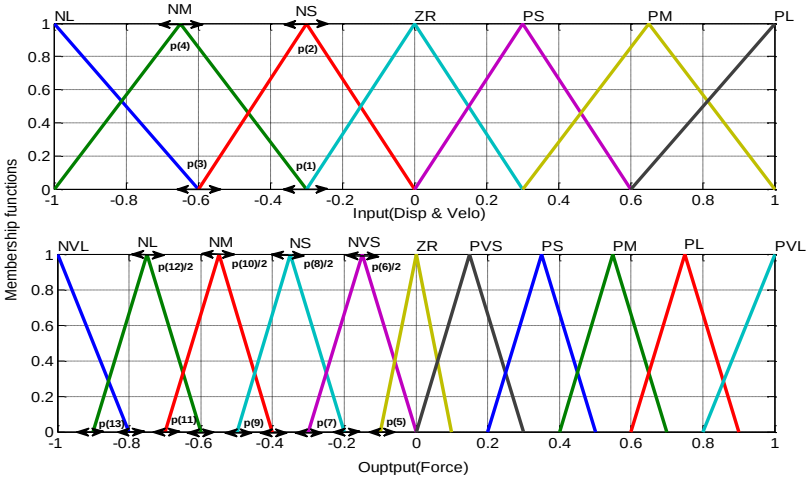

Fig. 10. Input and output membership functions

The fuzzy rule base is determined to represent the relationship between input and output fuzzy variables, where the output varies in proportion to the scale of each given input. The rule-base module is constructed by specifying a set of if -premise-then-consequent statements. For example, the multiple-input multiple-output IF–THEN rules of the fuzzy control are shown in the form:

$$R^j: \quad If\ x_1 is A_1^j\ and \cdots and\ x_p is A_p^j \quad Then\ \ y_1 is B_1^j\ and \cdots and\ \ y_m is B_m^j \tag{13}$$

where R j denotes the j-th rule of the fuzzy inference rule, j =1,2, . . . ,q, x1, x2, . . . , xp are the inputs of the fuzzy controller, A_i^j is the linguistic value with respect to xi of rule j , y1, y2, . . . , ym are the outputs of the fuzzy controller and $B_i^j$is a fuzzy singleton function defined by experts. Table 3 represents the fuzzy rule table used for the semi-active fuzzy controller in this study. The defuzzification module, the last component of the fuzzy logic, operates on the fuzzified outputs obtained from the inference mechanism. As noted earlier, we adopt the center of gravity (COG) defuzzification method in this study.

Table 3. Rule base table of fuzzy controller

Data base		Velocity						
		NL	NM	NS	ZR	PS	PM	PL
Displacement	NL	PVL	PL	PM	PM	PM	PS	PVS
	NM	PL	PM	PS	PS	PS	PVS	ZR
	NS	PM	PS	PVS	PVS	PVS	ZR	ZR
	ZR	PS	PVS	ZR	ZR	ZR	NVS	NS
	PS	ZR	ZR	NVS	NVS	NVS	NS	NM
	PM	ZR	NVS	NS	NS	NS	NM	NL
	PL	NVS	NS	NM	NM	NM	NL	NL

c) Optimization of FLC

GA optimally establishes a reasonable fuzzy correlation between the selected structural responses and the corresponding control forces provided by FDSAB. Consequently, GA is employed as an adaptive method for optimizing the FLC system according to a fitness function that specifies the design criteria in a quantitative manner. The displacement response of the stories due to earthquake excitation is taken as objective of the optimization problem, which should be minimized in the fitness function given by Eq. (11). In this stage, to design the GA-FLC, the fuzzy membership functions and rule base in fuzzy system are adjusted. In order to adjust the membership functions used for input and output variables, 13 parameters of P(1)-P(13), as shown in Fig 10, are considered in which, by using the GA optimizer, the performance of the designed FLC system can be optimized. All of the information represented by the FLC parameters is encoded in a chromosome which is made up of 13 genes representing these parameters. Due to symmetry, parameters of only half of the input and output membership functions, described earlier, have been considered as design variables. Figure 11 shows the final optimized membership functions for input and output vectors. Proper GA operator parameters are very important in improving the GA tournament. These parameters such as initial population size, crossover rate and mutation rate are chosen according to the problem type. In this stage, the number of initial population size is taken to be about 40. The crossover rate and mutation rate are taken as 0.85 and 0.01, respectively. The constraint of convergence is considered as 100 generations of the population.

The parameters of input and output membership functions should be optimized while the fuzzy rule base remains unchanged. After optimization of membership functions, the rules of the fuzzy controller are optimized based on the final membership functions. Since the table of rule bases is also symmetric, we shall optimize half of the rules that have been considered as design variables. Thus the rule base can be designed with 25 members of Table 3. Optimized rule base table of fuzzy controller is tabulated in Table 4. The final rule surface plot, after optimization, is shown in Fig 12. The number of initial population size

is taken to be about 50. The crossover rate, mutation rate and the constraint of convergence are taken as 0.85, 0.01 and 100, respectively, as the membership functions optimization.

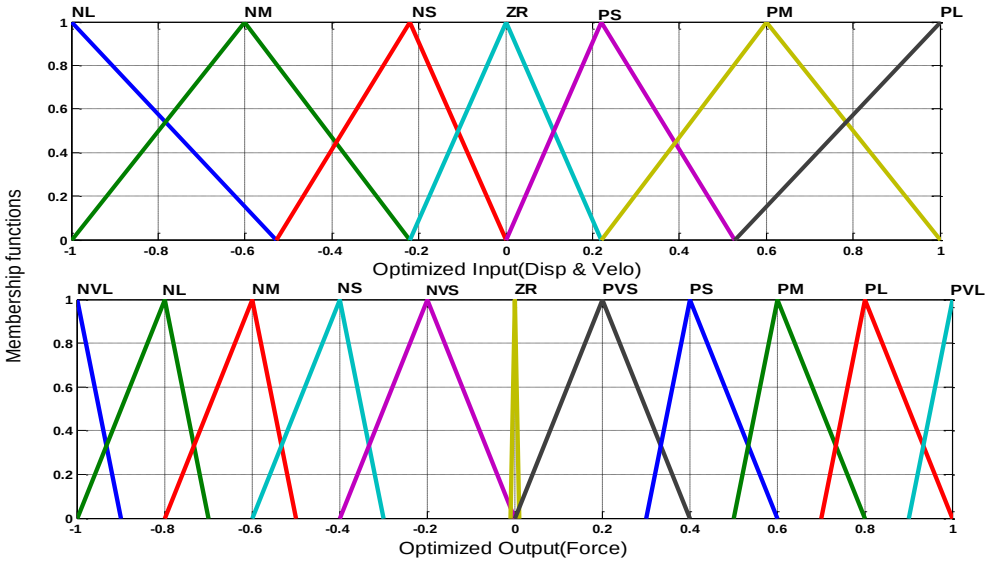

Fig. 11. Optimized Input and output membership functions

Table 4. Optimized rule base table of fuzzy controller

Data base		Velocity						
		NL	NM	NS	ZR	PS	PM	PL
Displacement	NL	PVL	PL	PM	PS	PVS	ZR	NVS
	NM	PL	PM	PS	PVS	ZR	NVS	NS
	NS	PM	PS	PVS	ZR	NVS	NS	NM
	ZR	PM	PS	PVS	ZR	NVS	NS	NM
	PS	PM	PS	PVS	ZR	NVS	NS	NM
	PM	PS	PVS	ZR	NVS	NS	NM	NL
	PL	PVS	ZR	NVS	NS	NM	NL	NL

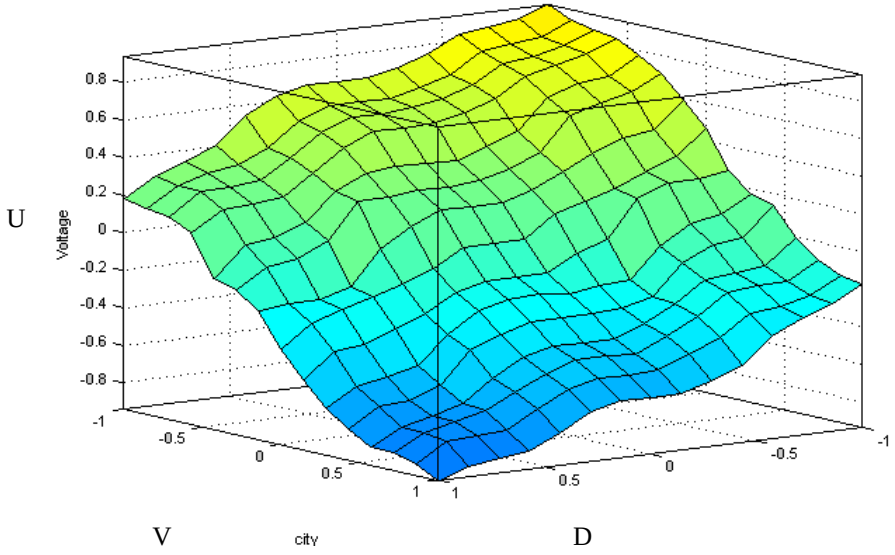

Fig. 12. Final representation of rule surface of fuzzy controller after optimization

d) Seismic response mitigation

To verify the control design validity and the effectiveness of described methods subjected to near-fault ground motions, time histories of roof displacement and profiles of drift are illustrated. For conciseness, graphic roof displacement and drift of the test structure are presented for only 3 of the 9 earthquakes considered. Nevertheless, discussion presented in this section will refer to structural responses to all 9 near-fault and far-fault seismic motions. Figures 13, 14 and 15 provide time histories of the roof displacement and drift for the uncontrolled structure compared with fuzzy-controlled and fuzzy-controlled compared with LQR control algorithm under the Northridge earthquake (SCS052) having forward directivity, Chi-Chi (TCU068EW) having fling step and Northridge (WST270) far-fault ground motion. For simplicity, in this paper, the seismic motion with forward directivity effect and fling step effect will be referred to as "FD" and "FS", respectively, while the far-fault seismic motion without pulse will simply be called "WP". As stated earlier, displacement response of the stories due to earthquake excitation is taken as objective of the control algorithm. Compared to the uncontrolled system, the fuzzy logic controlled FDSAB system greatly reduces the roof displacement in near-fault and far-fault earthquakes. The performance of the system employing the semi-active fuzzy control system surpasses that of LQR system in reducing roof displacement related to near-fault earthquakes. In near-fault having FS, it can be seen that the FLC significantly decreases the drifts. FLC performs better than LQR control system in reducing displacement responses subjected to FD, FS and yields in similar results for WP motions. As a result, the FDSABs reduce structural responses and are promising for semi active structural control in relation to characteristics of near-fault and far-fault fields.

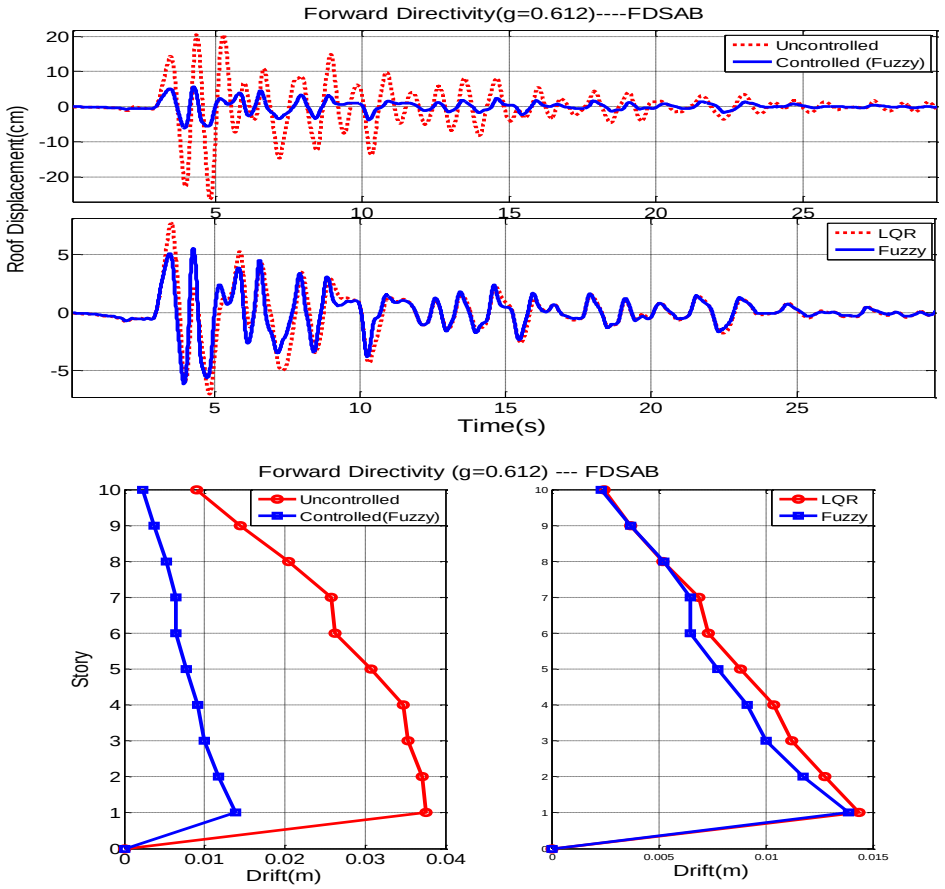

Fig. 13. Results of roof displacement time history and drift in controlled and uncontrolled structure-Forward Directivity (g=0.612)

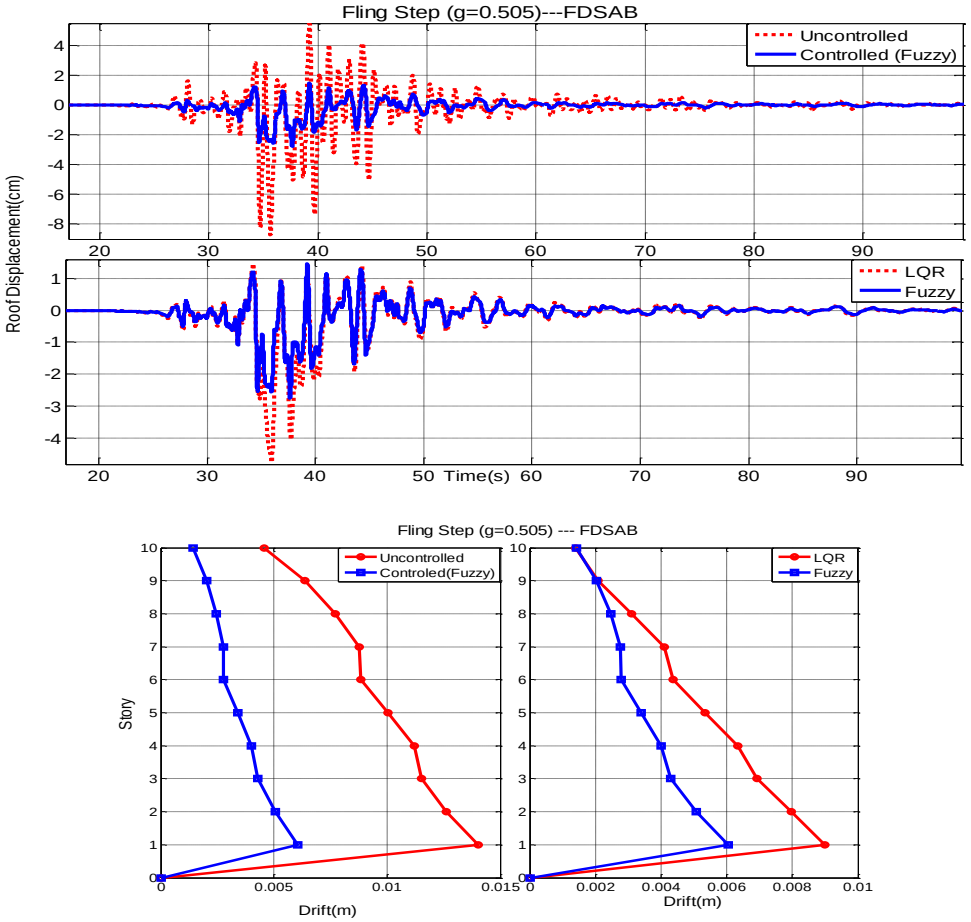

Fig. 14. Results of roof displacement time history and drift in controlled and uncontrolled structure – Fling Step (g=0.505)

The effectiveness of methods on response reductions in earthquake vibrations is further evaluated by a set of performance indices comparing the controlled response against the results obtained from the uncontrolled cases. There are different sets of evaluation criteria which are used in structural control to evaluate the performance of the buildings. The set of evaluation criteria used in this study to compare the performance of the structure are defined based on both maximum and RMS responses [26]. The first four criteria (J1, … J4) are based on peak responses:

$$J_1=\frac{\max\limits_{t,i}\left|\frac{d_i^c(t)}{h_i}\right|}{\max\limits_{t,i}\left|\frac{d_i^u(t)}{h_i}\right|} \qquad J_2=\frac{\max\limits_{t,i}\left|x_i^c(t)\right|}{\max\limits_{t,i}\left|x_i^u(t)\right|} \qquad J_3=\frac{\max\limits_{t,i}\left|\ddot{x}_{ai}^c(t)\right|}{\max\limits_{t,i}\left|\ddot{x}_{ai}^u(t)\right|} \qquad J_4=\frac{\max\limits_{t}\left|\sum_i m_i\ddot{x}_{ai}^c(t)\right|}{\max\limits_{t}\left|\sum_i m_i\ddot{x}_{ai}^u(t)\right|} \tag{14-17}$$

The next four criteria are defined in their normed based forms as:

$$J_5=\frac{\max\limits_{t,i}\left\|\frac{d_i^c(t)}{h_i}\right\|}{\max\limits_{t,i}\left\|\frac{d_i^u(t)}{h_i}\right\|} \qquad J_6=\frac{\max\limits_{t,i}\left\|x_i^c(t)\right\|}{\max\limits_{t,i}\left\|x_i^u(t)\right\|} \qquad J_7=\frac{\max\limits_{t,i}\left\|\ddot{x}_{ai}^c(t)\right\|}{\max\limits_{t,i}\left\|\ddot{x}_{ai}^u(t)\right\|} \qquad J_8=\frac{\max\limits_{t}\left\|\sum_i m_i\ddot{x}_{ai}^c(t)\right\|}{\max\limits_{t}\left\|\sum_i m_i\ddot{x}_{ai}^u(t)\right\|} \tag{18-21}$$

The last criteria is related to the control devices:

$$J_9 = \frac{\max_{t,l} |f_l(t)|}{W} \tag{22}$$

where xi(t) is displacement of i-th story, di(t) is drift of i-th story, $\ddot{x}_i(t)$ is acceleration of i-th story, $f_l(t)$ is control force produced by l-th device, mi is mass of i-th story, hi is height of i-th story and W is seismic weight of building. The term 'c' refers to the controlled system and the term 'u' refers to uncontrolled system. The norm, $\|u\|$, is computed using the following equation:

$$\|u\| = \sqrt{\frac{1}{t_f}\int_0^{t_f} (u)^2 dt} \tag{23}$$

and t_f is a sufficiently large time to allow the response of the structure to attenuate. The performance of the system according to set of evaluation criteria for seismic records characterized with forward directivity is tabulated in Table 5 for both FLC and LQR control methods. Table 6 provides comparative results of the evaluation criteria for the near-fault ground motions having fling step. In addition, the control performance of the semi-active FLC control strategy can clearly be observed from the simulation results for the far-fault ground motions listed in Table 7. Considering the overall evaluation criteria of far-fault motions, the FLC control system gives satisfactory results for the seismic response control in far-fault seismic motions and the values of evaluation criteria show very competent control performance in comparison with LQR method.

The effectiveness of the logic-based semi-active FDSAB system is verified from the evaluation criteria for the nine earthquakes given in Table 5 through Table 7. For evaluation criteria J1 and J5 (peak and RMS drift), FLC yields more reduction than LQR control method for the near-fault motions and performs close to LQR method for far-fault motions. Results of J2 and J6 (peak and RMS displacement) show that the control performance of the FLC is superior to LQR control method in near-fault earthquakes. Results of J2 and J6 for WP seismic motions indicate competent control performance in comparison with LQR method. For J3 (peak acceleration), results of LQR algorithm lead to more suppression than FLC. Results of J4 and J8 (peak and RMS base shear) show that LQR controller is superior to FLC. For J7 (RMS of acceleration), FLC results in less reduction than LQR control algorithm in relation to all of the seismic motions.

Table 5. Evaluation criteria of near-fault ground motions with forward directivity effects

	PGA=0.439		PGA=0.612		PGA=0.838	
	Fuzzy	LQR	Fuzzy	LQR	Fuzzy	LQR
J1	0.5390	0.4849	0.3695	0.3822	0.5356	0.4476
J2	0.3636	0.3929	0.2333	0.2916	0.5169	0.4183
J3	0.8187	0.7550	0.5606	0.3175	0.6442	0.5155
J4	1.0149	0.9566	0.5705	0.4254	0.5202	0.4781
J5	0.5471	0.6775	0.3527	0.3739	0.4669	0.4122
J6	0.4008	0.5899	0.2610	0.2993	0.4270	0.3617
J7	0.6252	0.5709	0.3581	0.2717	0.5052	0.3607
J8	0.8046	0.7193	0.3896	0.3302	0.5158	0.3969
J9	0.0326	0.0313	0.0451	0.0414	0.0401	0.0427

Table 6. Evaluation criteria of near-fault ground motions with fling step effects

	PGA=0.171		PGA=0.365		PGA=0.505	
	Fuzzy	LQR	Fuzzy	LQR	Fuzzy	LQR
J1	0.4116	0.5367	0.3644	0.4704	0.4310	0.6403
J2	0.3079	0.4936	0.2731	0.4190	0.3177	0.5498
J3	0.4770	0.4053	1.0366	0.9628	0.7191	0.6890
J4	0.4952	0.4575	1.1985	1.1330	0.9148	0.8851
J5	0.4782	0.5537	0.5062	0.6573	0.5053	0.6644
J6	0.3710	0.4789	0.3683	0.5727	0.3759	0.5831
J7	0.3482	0.3143	0.3701	0.3243	0.4401	0.4202
J8	0.4102	0.3903	0.4620	0.4183	0.5845	0.5395
J9	0.0211	0.0118	0.0211	0.0249	0.0211	0.0200

Table 7. Evaluation criteria of far-fault ground motions without pulse

	PGA=0.361		PGA=0.435		PGA=0.638	
	Fuzzy	LQR	Fuzzy	LQR	Fuzzy	LQR
J1	0.5387	0.4907	0.6201	0.6211	0.4322	0.3435
J2	0.3596	0.3196	0.4222	0.3788	0.2471	0.2453
J3	0.5095	0.4625	0.8120	0.7619	0.8115	0.8132
J4	0.7737	0.6962	0.9171	0.8748	0.9949	0.9543
J5	0.5110	0.4979	0.4666	0.4767	0.4024	0.3750
J6	0.3341	0.3026	0.3129	0.3050	0.2709	0.2533
J7	0.6272	0.5976	0.7388	0.7325	0.6814	0.6694
J8	0.8989	0.8569	1.0049	0.9970	0.9053	0.8786
J9	0.0211	0.0217	0.0167	0.0173	0.0221	0.0211

Seismic response mitigation of corresponding evaluation criteria, J1, J5 (peak and RMS drift) J2, J6 (peak and RMS displacement) exhibit less reduction subjected to near-fault motions having FD and FS effects. This point is illustrated in Fig 16 in which near-fault seismic motions present larger value of evaluation criteria than far-fault motions based on LQR control method. One noteworthy point is that near-fault earthquakes investigated in this study require larger control force (J9), especially for those having FD effect. Consequently, near-fault motions have potentially more influence on the seismic response mitigation and control of structure. Also, as shown graphically in Fig 16, seismic motions having FS effect present larger evaluation criteria indicating less response suppression than earthquakes having FD effect. In other words, near-faults motions characterized with FS affect the control of structure more intensely. It should be mentioned that fuzzy logic controller with FDSABs demonstrated high efficiency and yielded significant reduction in structural seismic response under various excitations.

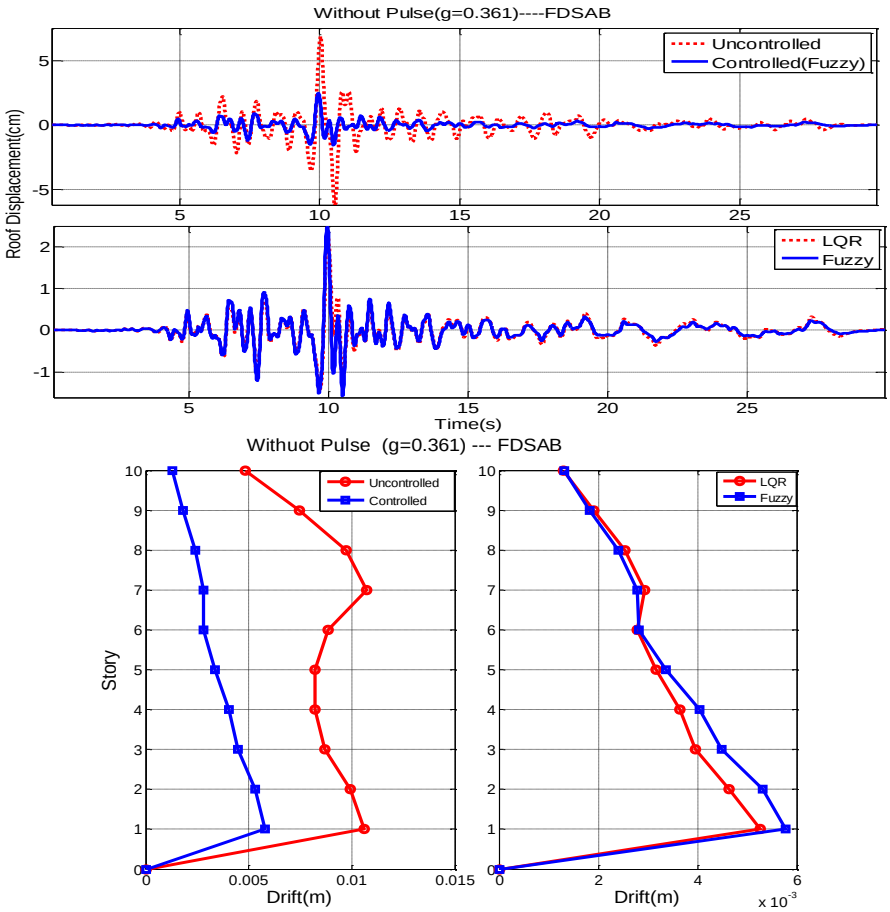

Fig. 15. Results of roof displacement time history and drift in controlled and uncontrolled structure – Far-fault motions (g=0.361)

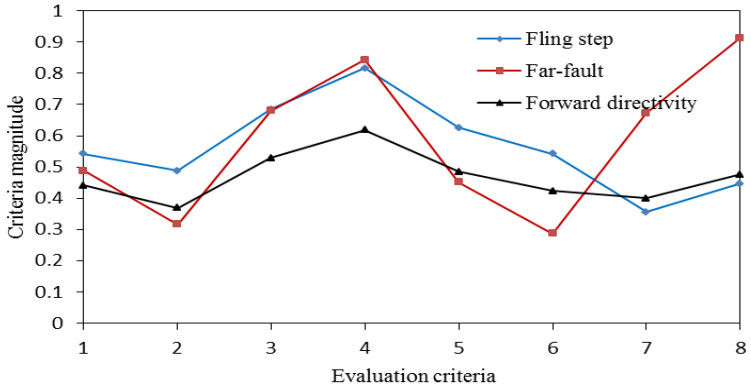

Fig. 16. Average of evaluation criteria for near-fault and far-fault ground motions

7. CONCLUSION

In this paper, a fuzzy rule-based control strategy for building frames equipped with friction damping system with amplifying braces was presented to evaluate structural control when subjected to near-fault seismic motions characterized with forward directivity and fling step in comparison with far-fault earthquakes. Displacement and velocity responses are considered as two input variable to the fuzzy logic controller. Results showed that the developed semi-active fuzzy controller was capable of reducing the displacement responses of the structure better than that of LQR control algorithm during near-fault earthquakes, therefore exhibiting a robust behavior to changes in external excitations. It was shown that

near-fault motions demand larger control force than far-fault motions, especially for records associated with forward directivity. Displacement response control resulted in larger reduction under far-fault ground motions compared to near fault earthquakes. In particular, ground motions having fling step effect demonstrated high influence and less response mitigation than forward directivity effect. The results of this investigation indicate the prospective use of fuzzy logic controller with FDSABs as semi-active devices in smart structures excited with near-fault motion characteristics.

REFERENCES

1. Gaul, L., Hurlebaus, S., Wirnitzer, J. & Albrecht, H. (2008). Enhanced damping of lightweight structures by semi- active joints. *Acta Mech*., Vol. 195, pp. 249-61.
2. Yi, F., Dyke, S. J., Caicedo, J. M. & Carlson, J. D. (2001). Experimental verification of multi-input seismic control strategies for smart dampers. *J Eng Mech*., Vol. 127, No. 11, pp. 1152–1164.
3. Casciati, F., Magonette, G. & Marazzi, F. (2006). *Technology of semi active devices and applications in vibration mitigation*. Chichester: Wiley & Sons.
4. Gluck, J. & Ribakov, Y. (2001). Semi-active Friction System with Amplifying Braces for Control of MDOF Structures. *The structural design of tall and special buildings*, No. 10, pp. 107-120.
5. Zhang, J. & Roschke, P. N. (1999). Active control of a tall structure excited by wind. *J Wind Eng Ind Aerodyn*., Vol. 83, pp. 209–223.
6. Dyke, S. J. & Spencer, B. F. Jr. (1997). Comparison of semi-active control strategies for the MR damper. In *Proceedings of the international conference on intelligent information systems*, Bahamas.
7. Jansen, L. M. & Dyke, S. J. (2000). Semi-active control strategies for MR dampers: comparative study. *Journal of Engineering Mechanics* (ASCE), Vol. 126, No. 8, pp. 795–803.
8. Paraskevopoulos, P. N. (2002). *Modern control engineering*. Marcel Dekker, Inc.
9. Zhou, L., Chang, C. C. & Spencer, B. F. Jr. (2002). Intelligent technology-based control of motion and vibration using MR dampers. *Earthq Eng Eng Vib.*, Vol. 1, No. 1, pp. 100–110.
10. Zahrai, S. M. & Shafieezadeh, A. (2009). Semi-active control of the wind-excited benchmark tall building using a fuzzy controller. *Iranian Journal of Science & Technology, Transaction B, Engineering*, Vol. 33, No. B1, pp. 1-14.
11. Xu, Z. D., Shen, Y. P. & Guo, Y. Q. (2003). Semi-active control of structures incorporated with magnetorheological dampers using neural-networks. *Smart Mater Struc*., Vol. 12, pp. 80–87.
12. Choi, K. M., Cho, S. W., Jung, H. J. & Lee, I. W. (2004). Semi-active fuzzy control for seismic response reduction using magnetorheological dampers. *Earthq Eng Struc Dyn*., Vol. 33, pp. 723–736.
13. Zahrai, S. M. & Salehi, H. (2014). Semi-active seismic control of mid-rise structures using magneto-rheological dampers and two proposed improving mechanisms. *Iranian Journal of Science & Technology, Transactions of Civil Engineering*, Vol. 38, No. C1, pp. 21-36.
14. Datta, T. K. (2003). A state-of-the-art review on active control of structures. *ISET, Journal of Earthquake Technology*, Vol. 40, No. 1, pp. 1-17.
15. Bidokhti, K. K., Moharrami, H. & Fayezi, A. (2012). Semi-active fuzzy control for seismic response reduction of building frames using SHD dampers. *Structiral Control and Health Monitoring.* Vol. 19, No. 3, pp.417-435.
16. Ozbulut, O. E., Bitaraf, M. & Hurlebaus, S. (2011). Adaptive control of base-isolated structures against near-field earthquakes using variable friction dampers. *Engineering Structures*, Vol. 33, pp. 3143–3154.
17. Kalkan, E. & Kunath, S. K. (2006). Effects of fling step and forward directivity on seismic response of buildings. *Earthquake spectra*, Vol. 22, pp. 367-390.

18. Ghaffarzadeh, H., Dehrod, E. A. & Talebian, N. (2013). Semi-active fuzzy control for seismic response reduction of building frames using variable orifice dampers subjected to near-fault earthquakes. *Journal of Vibration and Control*, Vol. 19(13), pp. 1980-1998.
19. Ghaffarzadeh, H. (2013). Semi-active structural fuzzy control with MR dampers subjected to near-fault ground motions having forward directivity and fling step. *Smart Structures and Systems*, Vol. 12, No. 6, pp. 595-617.
20. Somerville, P. (2002). Characterizing near-fault ground motion for the design and evaluation of bridges. *Proceedings of the 3rd National Seismic Conference and Workshop on Bridges and Highways*, 28, April–1 May, Portland, OR, pp. 137–148.
21. Somerville, P., Smith, N. F., Graves, R. W. & Abrahamson, N. A. (1997). Modification of empirical strong ground motion attenuation relations to include the amplitude and duration effects of rupture directivity seismological. *Research Letters*, Vol. 68, No. 1, pp. 199-222.
22. Cheng, F. Y., Jiang, H. & Lou, K. (2008). *Smart structures innovative systems for seismic response control*. CRC Press
23. Kim, Y., Hurlebaus, S. & Langari, R. (2010). Model-based multi-input, multi-output supervisory semi-active nonlinear fuzzy controller. *Comput-Aided Civ Infrastruct Eng*., DOI:10.1111/j.1467-8667.2009.00649.x.
24. Karr, C. L. (1991). Design of an adaptive fuzzy logic controller using a genetic algorithm. In *Proc of the 4th int'l Conf on Genetic Algorithms*, pp. 450–7.
25. Mohammadian, M. & Stonier, R. J. (1995). Fuzzy logic and genetic algorithms for intelligent control and obstacle avoidance. *Complexity International*, Vol. 2.
26. Ohtori, Y, Christenson, R. E. & Spencer. Jr. BF. (2004). Benchmark control problems for seismically excited nonlinear buildings. *Journal of engineering mechanics, ASCE*, Vol. 130, No. 4, pp. 366-385.